WELDING RESEARCH

SUPPLEMENT TO THE *WELDING JOURNAL,* OCTOBER 2007
Sponsored by the American Welding Society and the Welding Research Council

Response of Exothermic Additions to the Flux Cored Arc Welding Electrode — Part 1

Effectiveness of exothermically reacting magnesium-type flux additions was investigated with the flux cored arc welding process

BY S. H. MALENE, Y. D. PARK, AND D. L. OLSON

ABSTRACT. Flux cored arc (FCA) welding electrodes were fabricated with mixtures of magnesium and hematite flux. The heat input of welds from these electrodes were calorimetrically evaluated at several melting rates and resulted in peaks in heat input values. Exothermic reaction additions to the flux of the FCA welding consumable electrode demonstrated significant increases in arc process efficiency. The maximum efficiency was shown to occur at approximately 30 wt-% magnesium addition. The FCA welding process has shown higher measured heat input than the shielded metal arc (SMA) welding process for all of the wt-% ranges studied (10–50% in steps of 10%). Exothermic additions to the flux in the FCA welding process corrected the problem of uncontrolled chemical reaction as experienced with similar additions to the electrode coating of the SMA welding process. An exothermic addition at 30 wt-% Mg plus hematite, which replaced the iron powder of a baseline flux formulation, reduced the electrical dependence of the welding process by 50%. Studies in Part 1 showed the promise of exothermic-assisted FCA welding consumables and identified the upper limit in the melting rate for effective use of this exothermic-FCA welding electrode as being near 200 in./min (85 mm/s) for the fixed set of weld schedule parameters used. Part 2, investigation of exothermically reacting stoichiometric mixtures of aluminum, magnesium, and a 50/50 wt-% aluminum/magnesium flux additions in the FCA welding process, will be described in the following paper.

S. H. MALENE is with Savannah River National Laboratory, Aiken, S.C. Y. D. PARK is with Dong-Eui University, Dept. of Advanced Materials Engineering, Busan, Korea. D. L. OLSON is with Colorado School of Mines, Dept. of Metallurgical and Materials Engineering, Golden, Colo.

Introduction

Presently, field repair welding requires bulky dedicated electrical equipment and/or gas bottles with attendant torches, hoses, and regulators along with considerable operator skill. The electrical dependency can at least be minimized and the gas requirements eliminated with the proper incorporation of chemical heating reactions within the flux of contemporary flux-containing arc welding processes. A side benefit of a minimal arc dependency is a reduction in required operator skill level and a widening in the range of acceptable welding parameters. Portability and applicability will be enhanced with the concentration of chemical heat at the point of welding and with the reduction or near elimination of the welding process's dependence on electrical power.

The addition of energy, usually thermal energy, is necessary to overcome interfacial surface barriers in fusion welding. In conventional arc welding processes, this energy is supplied entirely by an electric arc. The flow of current through the local atmosphere between the electrode and workpiece generates plasma such that this energy is transferred to form a molten metal weld pool. Subsequent air cooling and conduction into the base metal results in the fusion and formation of the weld. In consumable welding processes, the electrode is designed to be consumed by providing the weld filler metal, and for FCA and SMA welding processes, a protective weld bead slag as well. Chemical dissociation and ionization of atmospheric species (including the consumables) within the arc are inevitable. If the types and amounts of chemical reactions can be controlled such that exothermic reactions predominate, then this chemical heat can supplant much of the heat of a conventional arc, theoretically to the point of obviating the need for the electric arc itself. The reaction of traditional thermite process mixtures, aluminum powder plus hematite (the mineral form of Fe_2O_3) and magnesium powder plus hematite, are known to produce enough heat energy to weld (Refs. 1–4). In such cases the welding operation is reduced to a "casting in place" technique.

In a previous investigation (Ref. 5) the heating potential of exothermic additions was characterized in the SMA welding process. In this process the flux is bonded coaxially along the outside of a consumable steel-rod electrode and tended to burn up and away from the arc, limiting the effectiveness of the exothermic additions at the electrode tip. To address this problem, encountered in the SMA welding research, of premature melt back of the flux along the outside of the electrode due to uncontrolled exothermic reactions, the FCA system was utilized. It was hoped to quantify, in a useful way, the implementation of these kinds of chemical heat sources into the more accommodating FCA welding system. It was the intent of

KEYWORDS

Consumable
Electrode
Exothermic Reaction
Flux Cored
Magnesium

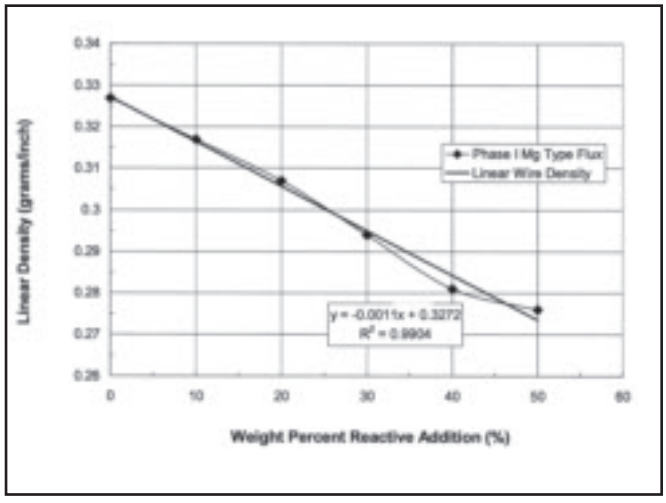

Fig. 1 — Electrode linear density as a function of wt-% magnesium-type flux addition for Part 1 study.

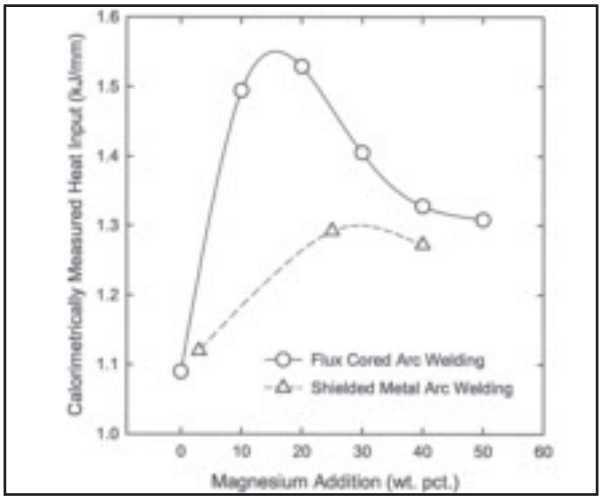

Fig. 2 — Calorimetrically measured heat input as a function of percent reactive addition for magnesium-type flux. The measured heat input of FCA and SMA welding are shown in one graph for comparison.

this investigation to evaluate the effective use of chemical heat in arc welding, particularly in the self-shielded FCA welding system. With the exothermic additions encased within the tubular sheath and shielded from atmospheric oxygen, opposite the case with the SMA system, it was anticipated that the added chemical heat reactions would come under control.

Another possible outcome was for the exothermic reactions, once initiated, to simply carry on within the sheath until the source reactants became exhausted. This outcome turns out not to have been the case. All of the flux formulations remained stable while in the wire electrode form once the electrical power was removed. On occasion a bit of expulsion was produced in the form of a ball of solidified dross at the end of the electrode stick-out. The spooled wire electrodes have remained stable while in normal storage conditions since their creation in the late 1990s. Care was exercised in the laboratory when dealing with the industrially pure powders in accordance with the use cautions specified in the attending material safety data sheets. All of the flux formulation powders represent a flash fire hazard when exposed to an ignition source such as an open flame when present in an unconfined manner.

The first objective of Part 1 was finding the effectiveness of exothermically reacting magnesium-type flux additions into the FAC welding process along with the refinement of the experimental procedures, and identification of the proper wire feed rate for these particular chemically assisted electrodes. The second objective was evaluating Part 1 electrodes as to their measured heat input with melting rates ranging from 200 to 300 in./min (85 to 127 mm/s) in steps of 25 in./min.

Table 1 — Flux Composition for Part 1 Electrodes, Parts by Weight-Percent

	Percent Reactive Addition for Magnesium Type Flux (wt-%)					
Ingredient	0	10	20	30	40	50
CaF_2	15	15	15	15	15	15
TiO_2	15	15	15	15	15	15
$CaCO_3$	6	6	6	6	6	6
SiO_2	4	4	4	4	4	4
Fe	60	50	40	30	20	10
Mg	0	6.7	13.4	20	26.6	33.4
Fe_2O_3	0	3.3	6.6	10	13.4	16.6

Experimental Procedures

A strip-to-tubular wire rolling mill was used to produce the electrodes with the different flux compositions for the Part 1 study. A set of five welding wires plus a baseline reference welding wire (0% additional exothermic content) was produced using magnesium and a fine commercial Fe_2O_3 powder (>325 mesh) as the hematite. The flux compositions for Part 1 are given in Table 1. The baseline self-shielded FCA welding flux formula, with a 60% wt-% iron powder concentration, was selected based on the works of Smith (Ref. 6) and Jackson (Ref. 7). The iron concentration was systematically displaced with a stoichiometric mixture of magnesium and hematite, three magnesium atoms to one hematite molecule. Steel strip was roll formed into a "u" shape and the flux was added. The "u" was closed into a tube sheath around the flux to form the flux-cored electrode wire. The wire was then drawn to 1/16-in. diameter, cleaned, and spooled. The strip used to form this sheath was AISI Type 1005 steel, 0.500 in. (12.7 mm) wide by 0.012 in. (0.3 mm) thick. The rolling mill was equipped with a computerized digital scale, a microprocessor motor controller, and an optical digital linear strip speed sensor integrated to allow for precise control and monitoring of the welding wire manufacturing process.

Electrode wires were produced with 17 to 18 wt-% flux fill to steel sheath ratios. A ½-in.- (12.7-mm-) thick by 2-in.- (50.8-mm-) wide bar stock of type AISI 1018 cold rolled steel was chosen as the base plate metal and cut into sample lengths of 5 in. (127 mm). A small wire was attached

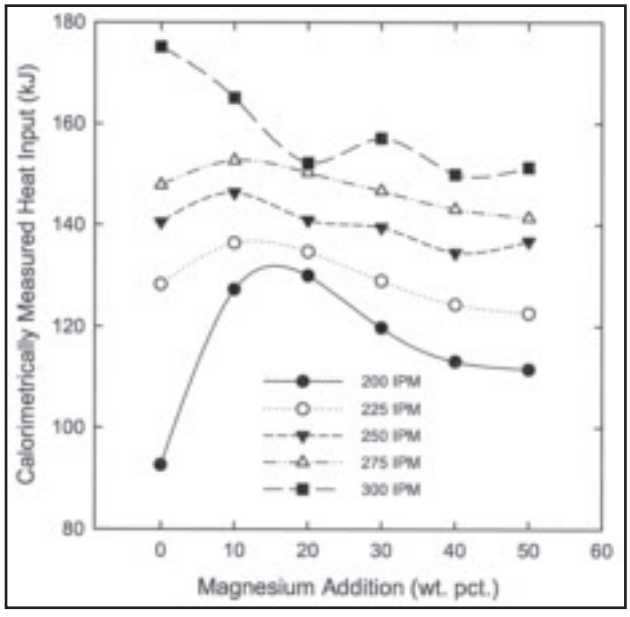

Fig. 3 — Calorimetrically measured heat input as a function of weight percent addition for magnesium-type flux at 200 to 300 in./min melting rate (85 to 127 mm/s).

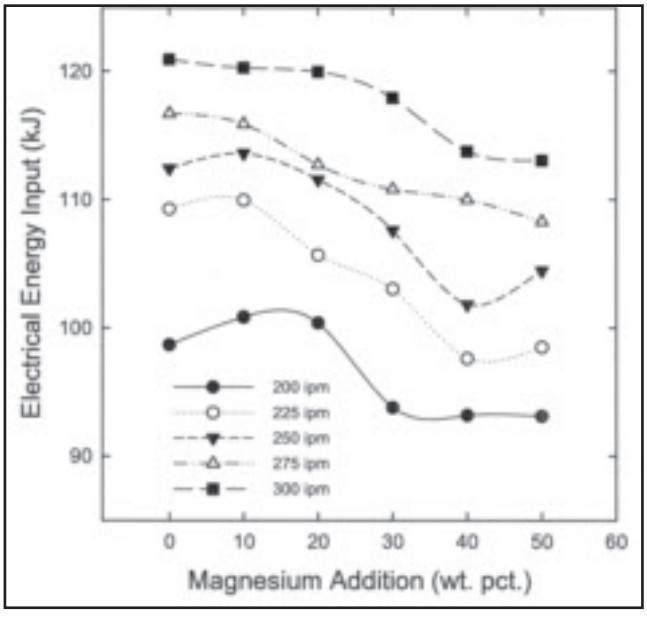

Fig. 4 — Electrical input energy as a function of weight percent addition for the magnesium-type flux at 200 to 300 in./min melting rate (85 to 127 mm/s).

to the edge of each sample to facilitate handling and suspension within the liquid nitrogen calorimeter dewar flask immediately following the test weld. The welding fixture consisted of three pins supporting the sample level in a horizontal plane with minimal contact area, longitudinally parallel to the direction of welding gun travel, with two bump-stop pins to hold alignment.

The test condition was as follows: 1) a single weld bead was placed bead-on-plate style along the center of the sample; 2) wire feed speed was varied between 200 and 300 in./min in steps of 25 in./min; 3) voltage was programmed on the machine for 25 V; 4) the weld was timed automatically for 20 s; 5) travel speed was held at 12 in./min (304.8 mm/min), resulting in a 4-in.- (101.6-mm-) long weld bead centered along the 5-in. (127-mm) sample length. Data collection consisted of measurement of the electrode extension length, deposit mass, heat input via calorimetry, welding current, and voltage. A minimum of five welding trials were conducted for each test condition. No microstructural, mechanical, or chemical evaluations were performed on the welds for this research.

A liquid nitrogen calorimeter was used to measure the amount of heat that was transferred into the base plate. The heat content of the sample is inferred by observing the change in the boil-off rate of a volume of liquid nitrogen for a period of time following the complete submersion of the welded sample within the liquid. Data acquisition software was used for acquiring the liquid nitrogen mass change data with time from the electronic scale. Calibration of the calorimeter was carried out by measuring the heat content of a pure copper test block and comparing the results with published data. The amount of nitrogen boiled off due to the sample is equal to the initial mass of the nitrogen (plus a buoyancy correction) minus the ending mass (corrected for normal ambient losses). A typical test sample would vaporize about 1000 g of liquid nitrogen in about 150 s, relating to approximately 140 kJ of measured heat. These measurements were accurate to within ± 5%.

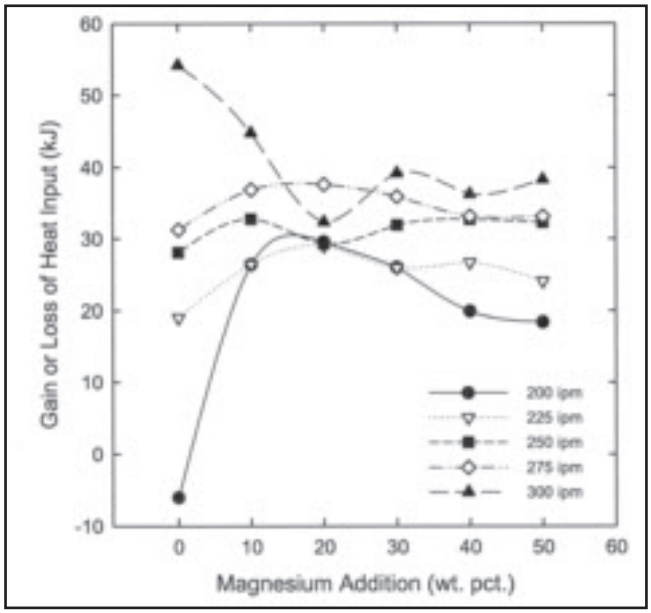

Fig. 5 — Gain or loss of heat input as a function of weight-percent addition for the magnesium-type flux at 200 to 300 in./min melting rate (85 to 127 mm/s).

The welding machine used in this investigation was a Miller Maxtron TM 450 in the CV (constant voltage) mode. The welding parameters were programmed and sample welds made with the selected electrode wire spool prior to welding on the samples. The welding sample was placed on the welding fixture with the contact-tube-to-work-distance (CTWD) preset to 0.75 in. (19 mm). The calorimeter was set up nearby on a cart and was started so that the scale under the dewar sent the mass change over time to the data acquisition computer and the results plotted on computer screen.

The Part 1 electrodes used a very fine, >325 mesh hematite, such that the packing density was dominated by the coarser, 150-mesh metal powders. The dense packing possible with the fine powder resulted

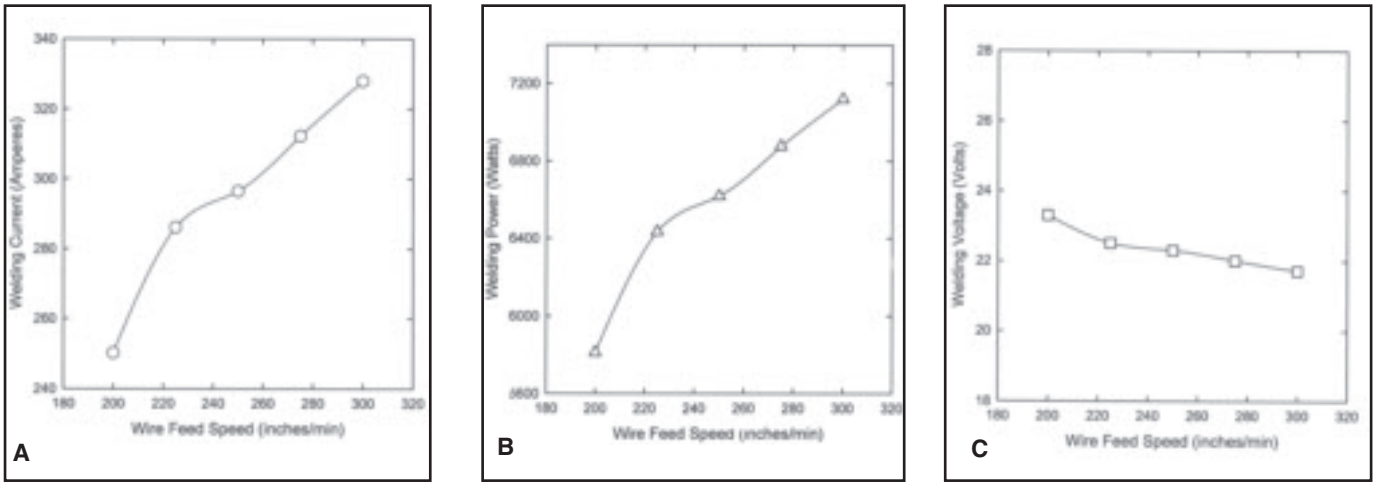

Fig. 6 — A — Welding current; B — welding power; C — welding voltage as a function of melting rate for the initial baseline composition electrode with no explicit exothermic flux addition.

in a slight systematic change in linear welding wire density for the fixed fill ratio employed. Figure 1 shows the Part 1 electrode linear density change as a function of weight percent magnesium flux addition. Although the weight percent fill, the ratio of flux mass to strip mass, was initially held constant during manufacture, the fixed geometry of the drawn wire outside dimension and the sheath thickness created a decrease in wire density as the magnesium thermite mixture displaces the iron powder going from zero to fifty percent. Although this density shift is not large on a mass basis, the effect is mentioned for the sake of completeness. Even at the 50 wt-% exothermic addition level, there is still 10 wt-% iron powder that can react with atmospheric or species added oxygen, or not. The thermodynamic effects of the flux formula reactions and the interplay with machine dynamic responses within the arc environment may belie what would be otherwise expected based simply on mass presence. The actual reaction path kinetics in the arc plasma is still not well understood.

Table 2 — Percent Calorimetrically Measured and Normalized (Dimensionless) Heat Input Change from Baseline Value

	Mg Flux (wt-%)				
Wire Feed Speed (in./min)	10	20	30	40	50
200	20.9	22.4	16.2	12.2	11.3
225	4.3	3.1	0.4	–0.2	–0.3
250	2.7	0.0	–0.7	–3.2	–2.0
275	2.3	1.3	–0.6	–2.2	–3.1
300	–0.5	–0.7	–2.5	–5.6	–6.4

Table 3 — Percent Normalized (Dimensionless) Electrical Welding Power Change from Baseline Value

	Mg Flux (wt-%)				
Wire Feed Speed (in./min)	10	20	30	40	50
200	2.6	1.9	–5.2	–5.5	–5.7
225	0.8	–3.4	–5.8	–10.7	–9.8
250	1.3	–0.9	–4.4	–9.6	–7.0
275	–0.6	–3.4	–5.1	–6.0	–7.4
300	–4.0	–9.2	–7.3	–10.3	–9.5

Results and Discussion

Calorimetrically Measured Heat Input

The primary interest in this flux formulation study was in the evaluation of the effects of chemical heat. No effort was made in fine tuning the formulation for commercial welding uses. As such it is not surprising that these electrodes, in some cases intentionally over loaded with thermite constituents, could not be made to form normal FCA weldments through the wire feed speed parameter manipulation alone. Also, because the weld test samples were immediately quenched in liquid nitrogen for calorimetric data, often the flux was interfused within the weld "overbead." Consequently, no typical weld morphological data was taken or is presented. The primary weld metric for this study is measured heat input, either due to the electrical energy consumed or the chemical energy liberated in the weld process. Figure 2 shows the peak in measured heat input with magnesium reactive additions to the welding wire flux, similar to the peak found in the SMA welding case (Ref. 5). A peak in the measured heat input is indicative of the optimal efficiency condition. As can be seen in the plot, the com-

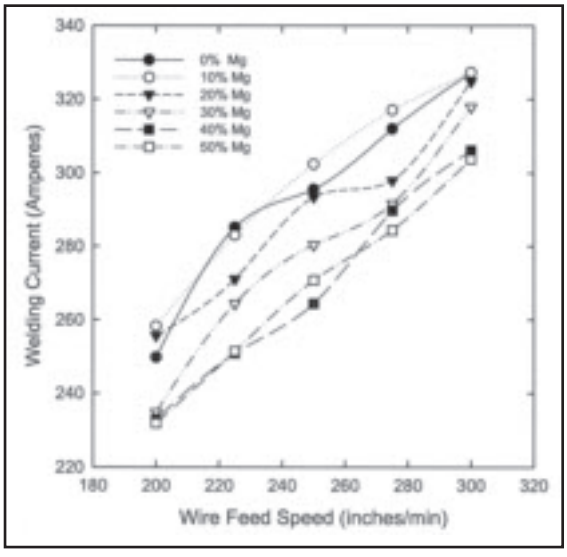

Fig. 7 — Welding current as a function of melting rate for the Part 1 magnesium-type flux-filled electrodes.

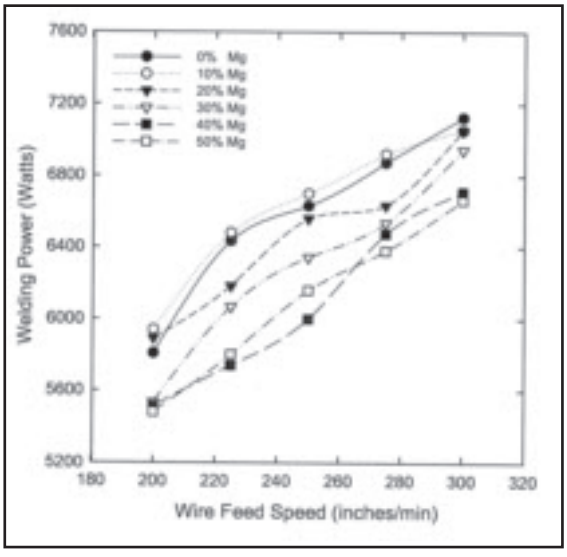

Fig. 8 — Welding power consumed as a function of melting rate for the Part 1 magnesium-type flux-filled electrodes.

parison of measured heat input between the FCA and SMA welding process clearly shows higher heat input in the FCA welding process. However, it is important to note in comparing the FCA and SMA results that SMA welding power supplies are of the constant current type and are fundamentally different from the continuous wire feed processes that are most typical of the constant potential, CP (also called constant voltage, CV) type. Although the process efficiencies are of the same range, the way in which these machine efficiencies may respond to "synthetic" heat additions within the arc are expected to be different. Thus, the ways in which the welding arc is electrically maintained may be fundamentally different for these two welding processes.

As the percentage of magnesium plus hematite in the flux of FCA electrodes increased, the arc was observed to get subjectively brighter. Obviously the magnesium was burning in the arc. Because the CTWD was kept constant and an increase in exothermic addition results in a decrease in steady-state electrode extension, the arc column length must increase with increasing magnesium addition for a given welding condition.

As the arc lengthens, the arc contact area with the sample surface workpiece becomes larger since the arc flares outward. For a constant electrical power setting, the energy density in this contact area decreases. Radiation losses increase to the point that although more heat energy is being generated through the arc with increasing exothermic flux concentration, less goes into the workpiece to be measured by the calorimeter. Less energy is likewise available to melt into the workpiece. The higher exothermic concentration electrodes, those above 20 wt-% Mg and not exhibiting a measured maximum heat input, may have further practical or experimental use at some other weld parameter setting. In other words, the weld parameter schedule used in this research was not optimized for any one particular flux composition. All compositions were evaluated with the same set of weld parameters.

Table 4 — Composite Net Gain Values (Normalized Dimensionless Energy Scalars)

	Mg Flux (wt-%)				
Wire Feed Speed (in./min)	10	20	30	40	50
200	18.3	20.5	21.4	17.7	17.0
225	3.5	6.5	6.2	10.5	9.5
250	1.4	0.9	3.7	6.4	5.0
275	2.9	4.7	4.5	3.8	4.3
300	3.5	8.5	4.8	4.7	3.1

At the fixed-torch heights used in the experiment, a peak in measured heat input was found at about 20 wt-% for the magnesium-type exothermic flux and 200 in./min (85 mm/s) melting rate. It is expected that lowering the CTWD or otherwise optimizing the welding parameters for each of the welding wires with higher exothermic concentrations would offset the increase in radiation losses incurred with longer arc lengths. It is conceivable that with high enough exothermic concentrations, a minimized arc could be maintained in a stable fashion, even with a slightly negative space CTWD, once the arc was established on the work surface and a large molten pool was formed. The jetting action of the arc and exothermic reaction forces could keep the molten weld pool depressed enough for this situation to be tenable. One would then expect a substantial increase in overall "arc" process efficiency as a large portion of the radiation would be captured that would otherwise be lost.

Increasing the wire feed speed is known to lengthen the electrode extension, thereby shortening the arc length for a fixed CTWD. A shortened arc length tends to constrict the arc and increase the energy density at the work surface. Further experiments were conducted with the initial batch of magnesium-type flux at increased wire feed speeds. Figure 3 shows the measured heat as a function of percent magnesium-type exothermic flux concentration for melting rates of from 200 to 300 in./min in steps of 25 in./min. The measured peak diminishes and shifts from

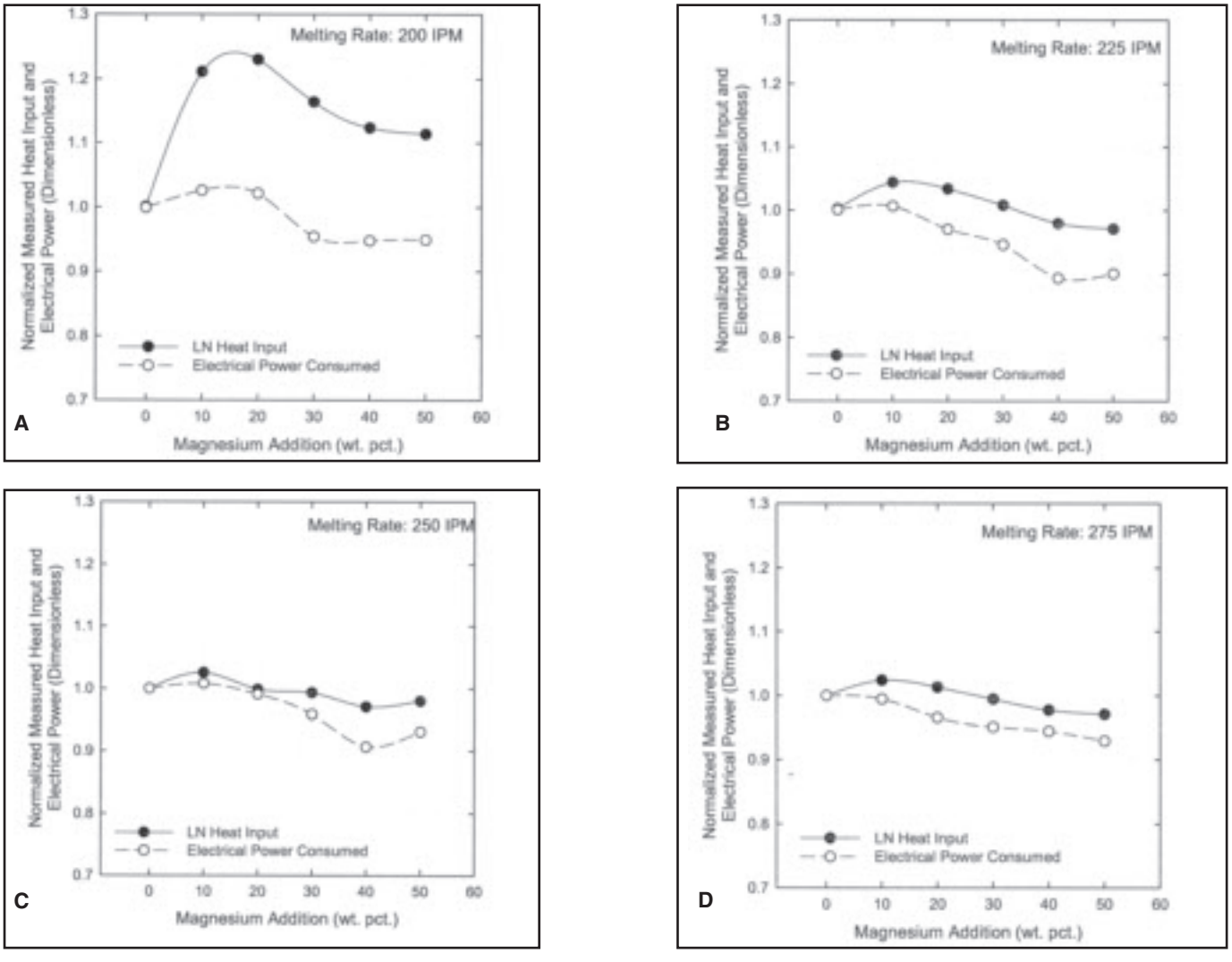

Fig. 9 — Normalized calorimetrically measured heat input and electrical power consumed for magnesium type flux at: A — 200 in./min (85 mm/s); B — 225 in./min (95 mm/s); C — 250 in./min (106 mm/s); D — 275 in./min (116 mm/s); E — 300 in./min (127 mm/s) melting rate.

about 20 wt-% back to about 10 wt-% addition as the melting rate increases. Perhaps the rapid vaporization and ejection of the molten metal and other constituents has a relative cooling effect on the arc, beyond the peak in process efficiency that compensates for the expected heat additions of higher concentration levels of exothermic flux constituents. Heat losses are also associated with spatter and all of the test welds in this batch were marked by excessive weld spatter.

Electrically Consumed Energy

Since the welding current goes up with melting rate for the CP machine used, it is expected that the measured heat input also increases with an increase in wire feed speed. Digital machine voltage and current readings were taken into a computer spread sheet and the product of the voltage and current (Watts) was averaged over the weld time and totaled into Joules (electrically consumed). The electrical heat input was then calculated by taking consideration of heat losses by convection and radiation, which is accounted for by the arc efficiency factor. Arc efficiency is the heat energy transferred into the sample divided by the electrical energy generated by the arc. The arc efficiency factor measured and taken for this study was 0.85, which also happens to be a mean value for the GMA welding process. Of note is that arc efficiency terms are based on the average of the weld cross-sectional areas, the areas of the weld fusion zone where the metal (both base and filler metal) has melted and resolidified. The measured calorimetric heat inputs presented here include the heating of the plate beyond ambient conditions due to

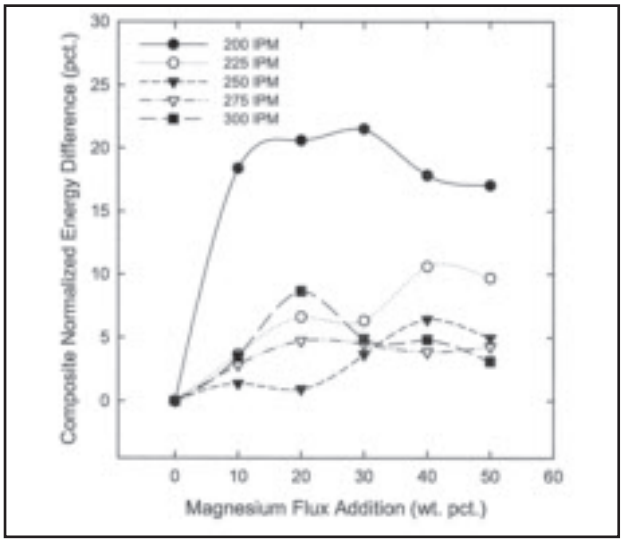

Fig. 10 — Difference in composite normalized energy value as a function of weight percent magnesium flux addition for the various melting rates.

electrical and chemical heat energy. Figure 4 shows the plotted results of measured electrical energy consumed as a function of reactive addition concentration level for the five wire feed speeds studied. Peaks were found in the measured electrical energy as a function of wt-% magnesium-type flux content. These plots look similar to those plots of the measured (electrical plus chemical) heat input as a function of exothermic flux concentration; however, the peaks are not located precisely at the same concentration levels.

Apparently the higher electrical heat input levels forced simply by an increase in wire feed speed (and hence current) mask to some extent the effects of the chemical heat additions. An optimal thermite concentration level is not detected with the higher melting rates since the appearance of peaks in measured heat inputs, above those increases attributed to that from electrical current alone, do not appear. As a subjective observation, the exothermic reactions are happening so violently (the arc looks brighter accompanied by much spatter) that the extra heat is simply being irradiated away and not conducting into the base plate. The peaks of the measured heat input and electrical power consumed most closely match each other in the 200 in./min case at between 10 and 20 wt-% magnesium-type flux concentration. The lower wire feed speed also produced the most realistic looking weld beads. For the baseline electrode condition (0% magnesium addition) electrode melting rates higher than 200 in./min do equate to measured gains of heat input as shown in Figs. 3 and 4. The larger amount of electrical heat associated with the higher current levels is being captured by the calorimeter, but some of the chemical heat is being lost. The calculated electrical heat input in kJ is then subtracted from the total measured heat input, also in kJ and the results are plotted in Fig. 5.

As shown in Fig. 5, for the baseline, zero percent flux addition case (with no added chemical heating), the total measured heat input minus that attributed to electrical energy is approximately a negative 8 kJ at 200 in./min and ranges up to about positive 55 kJ at the 300 in./min melting rate. Any heat measured above zero, once that amount due to electrical energy input at an assumed 100% transfer efficiency is subtracted, must be due to some kind of exothermic chemical reaction. In the case of no extra additions, it is believed that some of the 60 wt-% iron powder is oxidizing. The source of the oxygen can be from the atmosphere or from other flux constituents such as rutile (TiO_2), Calcium Carbonate ($CaCO_3$), or quartz (SiO_2). With the thermite additions, even the hematite (Fe_2O_3) may offer a source of oxygen for the iron powder since the oxidation/reduction of iron can take other alternative and presumed competing paths (FeO, Fe_2O_3,

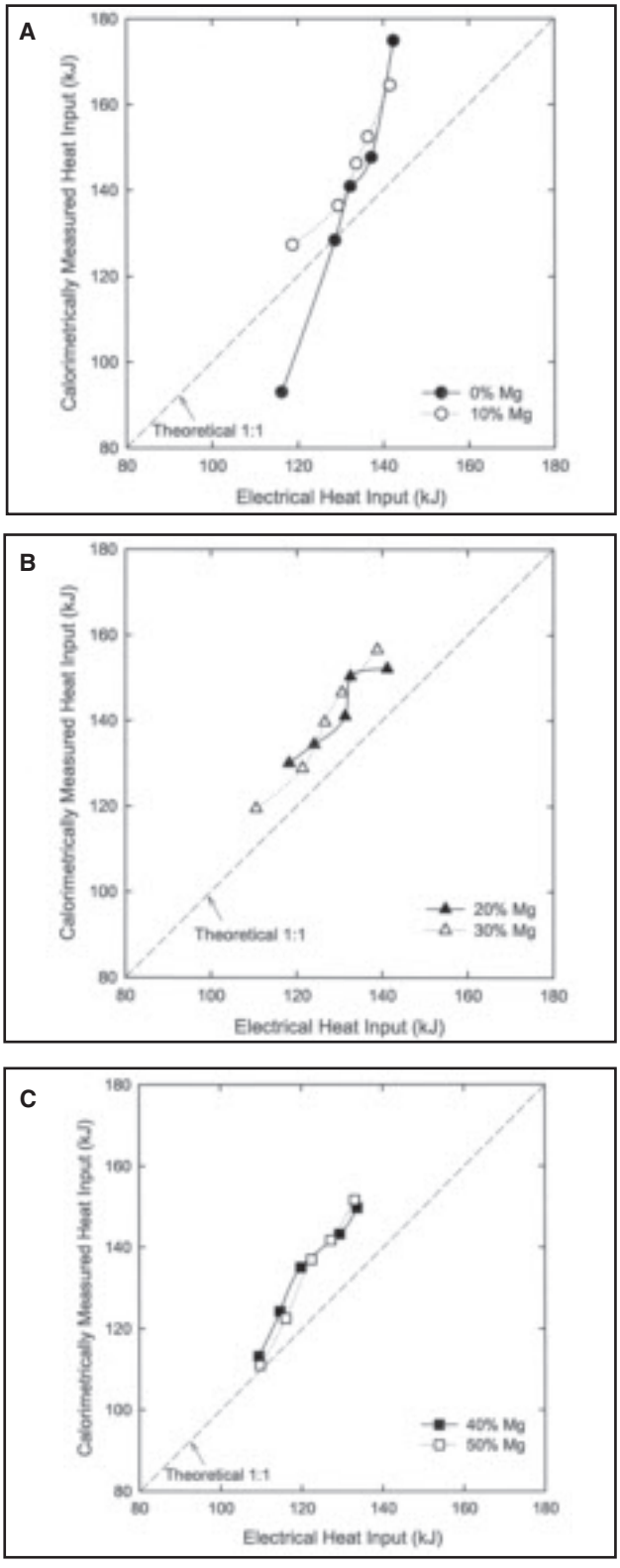

Fig. 11 — Calorimetrically measured heat input as a function of electrical heat input for: A — 0 and 10 wt-%; B — 20 and 30 wt-%; and C — 40 and 50 wt-% magnesium-type flux addition.

Fe_3O_4, etc.). Whatever the reasons for the measured heat input increases not directly attributable to electric power increases or the magnesium thermite additions, for the otherwise fixed welding parameters utilized in this study, the maximum benefit of this flux addition is shown to lie between 10 and 30 wt-% addition, and from 200 to 275 in./min electrode melting rate. It turns out that the baseline electrode flux formulation, consisting of 60 wt-% industrially pure iron powder, exhibits in and of itself exothermic properties when driven to excessive wire feed speeds. In addition to melting the iron powder for deposit filler, excessive electrical current associated with high feed rates may be contributing to the oxidation of iron constituents, and the liberation of chemical heat energy associated with such reactions. Note that not all of this heat energy as measured with calorimetry was actually used to form the fusion zone. While the fixed CTWD was short enough to collect the entire amount of weld spatter produced with the various feed rates, only the lowest feed rate tested produced a normal fusion zone. Feed rates lower than 200 in./min were not practical due to contact tube melt-back issues observed with the highest level of thermite addition.

Electrode Melting Rate as a Function of Welding Current, Voltage, and Power

In an effort to understand the confounding effects of electrical machine interplay with the chemical heat additions thought to be occurring within the arc environment, the welding current, voltage, and electrical power levels were plotted for the melting rates and flux concentration levels studied. Typically, the measured welding current for normal self-shielded FCA welding electrodes increases linearly with electrode feed rate. Figure 6A presents the average measured current values for the early baseline electrode (with no explicit exothermic flux addition) as a function of the set wire feed speed (melting rate). There is an inflection point at approximately 225 in./min (95 mm/s) electrode feed rate. Clearly some sort of mechanistic change in the arc process occurs here. Figure 6B shows the electrical power consumed in the weld as a function of set wire speed for the early baseline electrode. Because electrical power is the product of current and voltage, and a constant potential (CP) machine keeps the voltage relatively constant, then electrical power will scale with the current. A slight deviation from linearity for this baseline electrode is observed in the welding voltage as a function of melting rate (Fig. 6C), and an otherwise steady decrease in the measured voltage with wire feed speed is shown. Recall that the welding machine voltage was set at a fixed value of 25 V; for a fixed CTWD, an increase in wire feed speed will result in an increase in electrode extension and a shorter arc length. Voltage is proportional to arc length even for a given setting on the CP machine, yielding a decrease in voltage with an increase in melting rate. The nonlinear "bump" in both the current and voltage as a function of melting rate relationship is being attributed, to some extent, to the exothermic reactions in the arc. This is essentially the only variable that has been systematically changed.

Figure 7 depicts the welding current as a function of the wire feed speed for the six experimental electrodes of this study. The function for the 10 wt-% magnesium electrode is practically the same as that of the baseline electrode. The functions for the 40 and 50 wt-% electrodes are likewise similar to each other. Otherwise, in general for the mid-range concentration levels, the current required to maintain a given melting rate decreases with increasing exothermic concentration. Apparently, the higher concentration levels of reactive addition allow the electrode extension to melt back farther for a given electrical power setting than for the baseline (0 wt-% Mg) case. The self-regulation aspect of the FCA welding wire feed process therefore requires less current with more reactive addition than for the baseline (nonaddition) case.

Figure 8 reveals how the welding power consumed responded to the set melting rate for all of the electrodes. As can be expected, the plots are very similar to those plots for the welding current response depicted in Fig. 7. Subtle differences are due to the slight voltage variation in the melting rate among the various electrodes studied, even though a CP welding machine was used.

Normalized Measured Heat Input and Electrically Consumed Energy

Because the graphs of welding power and current as a function of weight percent fill exhibited peaks similar to the measured heat input (from the calorimeter) as a function of concentration, the data should be normalized to the baseline values of electrical power (current) and measured heat input. Creating such relative scales, in which the calorimetrically measured heat input value and the electrical power consumed for the baseline weld sample is unity, allows the differences due to explicit exothermic additions to be observed more clearly. Figure 9A is a plot of such normalized data at a melting rate of 200 in./min (85 mm/s) and clearly shows the effect of the exothermic flux addition on the measured heat input and the electrical power consumed.

At the 200 in./min (85 mm/s) melting rate, the 10 and 20 wt-% fluxes exhibited substantial increases in measured heat inputs (slightly more than 20%) over the baseline welds. The electrical power consumed also went up slightly (between 1 and 2%). The measured heat then dropped with increasing flux concentration (to about one percent above the zero addition baseline value) for the 40 wt-% flux addition.

The electrical power consumed also drops, to below the baseline value by about five percent for both of the higher concentration values. Perhaps the presence of the exothermic reactants is lowering the arc resistance at these concentration levels. Certainly, when consideration is given to the electrical properties of the physical combination of the electrode extension and the arc length as a whole (extending in one dimension the fixed distance of the CTWD), a reduction in electrode extension length believed to accompany exothermic flux additions must reduce the resistance contribution of the electrode. Concomitantly, of course, the arc must lengthen.

Because the welding voltage was held essentially constant by the power supply employed, the effects of the additions on the welding power are mainly through the welding current. These effects taper off with higher melting rates and are completely gone at 300 in./min (76 mm/s) for all concentration levels studied.

Figure 9B shows the normalized measured heat input and electrical power consumed for a melting rate of 225 in./min (95 mm/s) wire feed speed. At the 10 wt-% flux addition level, the measured heat increase of about five percent over the baseline is much less than the twenty percent value for the 200 in./min (85 mm/s) case while the electric power consumed remains practically unchanged from the baseline value. At 20 wt-% addition, the measured heat increase was about four percent over the baseline while the electrical power consumed dropped by approximately four percent. At 30 wt-% addition, the measured heat input is the same as that for no addition while the electric power consumed is slightly more than five percent below the baseline value. Again, the results for the 40 and 50 wt-% additions are practically the same as each other; however, in this case the measured heat input values are actually reduced below that of the baseline value, by slightly less than four percent. The electrical power consumed is a full ten percent less than the baseline value. In this melting rate region at the higher two concentration levels the exothermic additions result

primarily in a reduction of electrical power consumed rather than in a measurable increase in heat input directly.

Figure 9C shows the normalized results for the 250 in./min (106 mm/s) melting rate. The beneficial heat effects of the exothermic additions are not observed at all for the 10 and 20 wt-% concentrations. The slight, perhaps two percent, increase in measured heat input at the 10 wt-% level is practically offset by the one percent rise in electrical power consumed. The 20 wt-% values at this melting rate are indistinguishable from those of the baseline for both power and heat input. The 30 wt-% addition at this melting rate also reveals no measurable heat input change from that of the baseline. The electrical power consumed for this 30 wt-% data set reveals, however, a five percent reduction in electrical power from the baseline value. At 40 wt-% a maximum of ten percent reduction in power consumption is recorded along with a reduction in measured heat input of about four percent. The 40 wt-% data set shows only about a two percent reduction in measured heat input while the power consumed is reduced by seven percent.

Figure 9D shows the results for the 275 in./min (116 mm/s) melting rate. Both the normalized measured heat input curve and the normalized electrical energy consumed curve are relatively flat with the unity value line of the baseline weld. Only the 10 and 20 wt-% values show an increase in measured heat input of about two and one percent, respectively. All other values in this figure are negative. The reduction in electrical consumption ranges from zero to about seven percent within the range of flux concentrations while the reduction in measured heat input goes from about zero (0.6%) at 30 wt-% to about three percent at 50 wt-%. The measured effects of the exothermic flux additions appear to be most benign at this 275 in./min (116 mm/s) melting rate. Little change in either measured heat input or electrical energy consumed is observed at this melting rate.

Finally, at 300 in./min (127 mm/s) wire feed speed, Fig. 9E shows practically no change in measured heat input for the 10 and 20 wt-% trials compared to the values recorded for the baseline electrode. For this wire feed speed, all measured heat inputs for the various weight percentages were less than that recorded for the baseline electrode. Likewise, for the electrical power consumed, all of the values recorded were below those corresponding to the baseline electrode, more so than at 275 in./min (116 mm/s). In the measured heat input case, the values decrease from an absolute minimal difference of minus 0.5% at 10 wt-% addition to an absolute maximum of minus 6.4% at 50 wt-% addition. The electrical power consumption at this melting rate, varied from an absolute minimal difference of minus 4.0% at 10 wt-% addition to an absolute maximum difference of minus 10.3% at 40 wt-% addition. Above the 200 in./min (85 mm/s) melting rate, the higher reaction rates of the exothermic additions allowed by the higher sheath melting rates simply leads to much higher radiation and spatter losses. Lower melting rates would likely better utilize and control slower exothermic reactions.

Net Gain Values Normalized Heat Input Benefit Plus Electrical Power Reduction

Because a reduction in the electrical power consumed, brought about for a given welding condition by the addition of chemical heating components, is likely to be as beneficial as a directly measurable increase in heat input (in Joules), a composite normalized energy scale, in relative percent, is composed. By subtracting the percent electrical power difference from the percent measured heat-input difference for each welding condition, a net gain value is calculated. The normalized dimensionless parameter values used to create this composite gain value are presented in tabular form.

Table 2 lists the measured heat inputs relative to the baseline value. The largest gain in measured heat input over the baseline value occurred with the 20 wt-% addition at 200 in./min melting rate with a 22.4% difference. The fact that the relative measured heat input generally goes down as the exothermic concentration level goes up can only partly be explained by the commensurate reduction in linear electrode density. While the exothermic flux compounds are lighter than the iron powder that they displace in the electrode core, in this regime replacing the pure metallic species iron, presumably having a known thermodynamic effect, with the other pure metallic species, whose thermodynamic effects are being studied, shows that the baseline iron is also a strong exothermic constituent. The relative measured heat input goes down with increasing melting rate can be explained by the fact that the arc process efficiency of the baseline electrode, to which these other electrodes are compared, increases substantially with melting rate, as shown later in Fig. 11.

Table 3 lists the percent normalized electrical welding power changes from baseline values. The largest reduction in electrical power consumed occurred at the 225 in./min melting rate for the 40 wt-% addition with a 10.7% reduction from the baseline value. The fact that the relative electrical welding power consumed generally goes down with increasing wire feed speed is best explained as being due to the corresponding decrease in arc length and hence welding voltage and electrical power. That the relative electrical welding power consumed generally goes down with increasing exothermic concentration level is believed to be due to the ease with which the electrode extension can burn back with exothermic additions and the self-regulating nature of the FCA welding CP power supply.

The largest composite gain, the percent measured heat input difference minus the percent electrical power difference (Table 4), occurred at 200 in./min melting rate and 30 wt-% fill with a 21.4 dimensionless composite normalized energy value. The huge gain in normalized measured heat input of over twenty percent in this concentration range far outweighs the concomitant reduction in electrical power consumption. The lower melting rate, the lowest tested in this investigation, garnered the highest overall benefit of the exothermic additions, probably due to the provision for the longest amount of time for nearly complete combustion of the pure metal additions.

The composite normalized energy value as a function of weight percent addition of Fig. 10 reveals again that at the 200 in./min (85 mm/s) melting rate, the lowest tested in this study, a significant increase from baseline values is recorded. By including the measured reduction in electrical power consumed with the measured increases in heat input via this normalized data, the maximum benefit of this early type magnesium flux is shown to occur at around 30 wt-% level rather than the 20 wt-% level for the measured heat input variable alone. An intermediate concentration level was not investigated.

Calorimetrically Measured Heat Input and Electrically Consumed Energy

Another way to view the thermal data of the Part 1 electrodes is to equate the equivalent energies of the calorimetrically measured heat inputs in kJ with the electrical heat inputs also in kJ. A theoretical one to one correspondence will result at 100% electrical arc process efficiency with no chemical heating.

Figure 11 is a plot of the calorimetrically measured heat input in kJ as a function of the electrical energy input (also in kJ). The data points are plotted in the order of increasing melting rate from 200 to 300 in./min in steps of 25 in./min (85 to 127 mm/s in steps of 10.5 mm). The most surprising aspect is that the bulk of the data plots above the 100% electrical efficiency (theoretical 1:1 ratio) line, even for

the baseline electrode. Realize that the base electrode contains 60 wt-% pure iron powder that itself reacts exothermically.

The deviation from the slope of the theoretical one to one ratio of electrical input energy to calorimetrically measured input energy is most notable for the baseline electrode throughout the melting rates studied. A steepening of the slope above that for the theoretical one-to-one ratio line is attributable to two primary causes. First, an increase in wire feed speed, for a fixed CTWD and other parameter settings, will lengthen the electrode extension and shorten the arc length, thereby increasing the arc process efficiency. Secondly, an increase in melting rate, for a fixed weld time, increases the amount of available chemical heat contributions of any exothermic flux constituents residing in the electrode. Without the benefit of explicit exothermic flux additions, the baseline electrode has less ability to melt back at the higher melting rates, thus explaining the slope variation.

The 10 wt-% magnesium electrode parallels the theoretical line until the 250 in./min melting rate, where it also undergoes a sudden steepening of slope. All the points of Fig. 11A plotted above the theoretical 100% electrical efficiency line (except for the baseline electrode at 200 in./min melting rate) and this is attributed to the chemical heat released through the exothermic reactions of the flux additions. The energy equivalency plots for the 20 and 30 wt-% electrodes are presented in Fig. 11B. Both electrode types follow the same slope as the theoretical ratio line for the first few data points and all points plotted above it. Both of the electrodes undergo an inflection point near the 250 in./min (106 mm/s) melting rate. The slope is then essentially flat for the last two (highest) melting rates tested for the 20 wt-% electrode but remains relatively constant and steeper for the 30 wt-% electrode. Higher melting rates equate to more chemical heat energy available with perhaps less time for the reactions to be fully utilized in the welding process. Higher melting rates also equate to longer electrode extension lengths with shorter arc lengths (with fixed CTWD). A higher melting rate usually means higher arc process efficiency and therefore more measurable heat input.

Radiation losses can undergo a step change if, for instance, the sample plate thickness is less than some critical value where the heat flow in the bulk of the plate transitions from three dimensional to two dimensional. Once the two-dimensional heat flow mechanism is invoked, the radiation losses can initially double. Heat can flow out of the sample from both the top and bottom surfaces. The baseline electrode with 60 wt-% iron is most efficient thermally at the highest melting rate tested and the explicit exothermic additions are made at the expense of iron powder concentration. The heats of formation for the various iron oxide compounds have combustion temperatures that more closely relate to the melting point of iron and, therefore, at least in bulk quantities, is perhaps more useful for heat production and heat transfer in the welding of steel than the "hotter reacting" magnesium-type thermite process. Energy equivalency plots for the 40 and 50 wt-% magnesium-type electrodes are presented in Fig. 11C. Both electrodes exhibit similar initial slope, steeper than that of the theoretical line, indicating an increase in heating efficiency with melting rate. Inflection points for both electrodes occur around the 250 in./min (106 mm/s) melting rate region whereupon the slope reverts back to about that of the theoretical ratio line. The positive effects of the exothermic additions are diminishing in both cases as the melting increases beyond 250 in./min (106 mm/s) and as the iron powder is further supplanted with exothermic ingredients. Perhaps the optimal recipe for efficient heat generation and transfer into the weld and the creation of sound weld bead morphologies will necessarily include an amount of pure iron powder.

Summary and Conclusions

Exothermic additions to the flux of the steel FCA welding consumable electrode have resulted in measurable increases in the arc process efficiency when consideration is given to the addition of chemical heat to the process often accompanied by a reduction in electrical energy consumed. The maximum benefit of this early type of magnesium flux was shown to occur at around the 30 wt-% level rather than at the 20 wt-% level for the measured heat input variable alone. The presence of iron powder is beneficial in moderating the exothermic flux reactions.

All melting rates studied in Part 1 produced a spray mode with a great deal of spatter. The slag was interfused into the surface quite tenaciously and very unevenly. The aggressive burning action of the magnesium in the arc likely prevented effective heat and metal transfer, as evidenced by the large amounts of surface spatter encountered. Also, the perceived shift in heat transfer mode from three-dimensional to two-dimensional beyond the 200 in./min (85 mm/s) set melting rate may have helped confound the heat input measurement issue. Thicker weld coupons and reduced power settings were used in Part 2 along with chemically more efficient stoichiometric ratios of exothermic flux ingredients.

Acknowledgments

The authors acknowledge and appreciate the support of the U.S. Army Research Office, Savannah River National Laboratory, and Dong-Eui University.

References

1. Jacoby, N. 1977. Principles and examples of application of aluminothermic pour-fusion welding. *PRAKTIKER* 29(5): 77–79.

2. Glushchenko, A. S. 1980. Determination of the productivity of the thermit arc-welding process under an exothermic flux. *Welding Production* 27(9): 37–39.

3. Krylov, Y. I., and Bronnikov, V. A. 1976. Thermite mixtures based on exothermic reactions of BN and Si_3N_4 with metals. UDC 669.018.45, Translated from *Poroshkovaya Metallurgiya*, 1(157): 52– 55.

4. Ioffe, I. S., Kuznetsov, O. M., and Piterskii, V. M. 1980. The effect of the titanothermite mixture included in the electrode coating on the increase in the productivity of welding. *Welding Production* 27 (3): 29–32.

5. Allen, J. W., Olson, D. L., and Frost, R. H. 1998. Exothermically assisted shielded metal arc welding. *Welding Journal* 68(7): 277-s to 285-s.

6. Smith, D. C. 1970. Flux-cored electrodes — their composition and use. *Welding Journal* 40 (7): 535 to 547.

7. Jackson, C. E. 1973. *Fluxes and Slags in Welding.* Welding Research Council Bulletin (190): 1–25.

8. Malene, S. H. 2000. Response of exothermic additions to the flux-cored arc welding consumable electrode. Ph.D. dissertation. Colorado School of Mines, Golden, Co.